Saudi Pharmaceutical Journal 31 (2023) 312–328

HOSTED BY

Contents lists available at ScienceDirect

Saudi Pharmaceutical Journal

journal homepage: www.sciencedirect.com

Review

SPECT/CT and PET/CT, related radiopharmaceuticals, and areas of application and comparison

Fawaz F. Alqahtani *

Department of Radiological Sciences, College of Applied Medical Sciences, Najran University, Najran, Saudi Arabia
Health Research Centre, Najran University, Najran, Saudi Arabia

ARTICLE INFO

Article history:
Received 17 November 2022
Accepted 27 December 2022
Available online 30 December 2022

Keywords:
Imaging
SPECT
PET
CT
Radionuclide
Nuclear medicine

ABSTRACT

The paper begins by identifying the key historical elements in the development of nuclear medicine imaging, focusing on the Anger camera and single photon emission computed tomography (SPECT) technologies. In this context, key reference is made to the physics of detection in Anger camera systems, especially key components such as the sodium iodide crystal, the function and performance of photomultiplier tubes, and the collimator design. It is discovered that within each component of technology, there are fundamental physical relationships that govern the performance of each component, and that overall image quality is the result of the complex interaction of all such elements. The increasing use of SPECT/CT imaging is described and illustrated with a range of typical clinical applications, which include brain, spinal, cardiac, and cancer studies. The use of CT imaging functionality allows for SPECT image correction based on compensation for absorption within tissue. Reference is also made to the basics of positron emission tomography (PET) imaging and, in particular, to the integration of PET/CT systems where the anatomy profile of the CT image is used to provide correction for photon absorption. A summary is provided of the radionuclides and radiopharmaceuticals commonly used in PET/CT imaging and a range of image studies referenced includes those of nasopharyngeal carcinoma, lung cancer investigation, brain investigation (cancer detection and dementia) and cardiac function. Reference is made to the development of "time of flight" (TOF) technology for improving of image resolution in PET/CT systems. Furthermore, SPECT/CT and PET/CT imaging systems are compared, where a key factor identified is the significantly higher number of photons detected with PET/CT technology and improved image resolution.

Contents

* Corresponding author at: Department of Radiological Sciences, College of Applied Medical Sciences, Najran University, Najran 1988, Saudi Arabia.
E-mail address: ffalqahtani@nu.edu.sa

Peer review under responsibility of King Saud University.

Production and hosting by Elsevier

https://doi.org/10.1016/j.jsps.2022.12.013

1. Introduction

A key element of modern medicine is the unprecedented ability to image the human body. The use of X-rays provides planar images, as dose CT tomography, where images are based on photon absorption. Magnetic resonance imaging (MRI) functions in the context of the nuclear magnetic dipole of hydrogen atoms, where images can be configured to identify specific tissue characteristics. The role of nuclear medicine is to provide an imaging modality that can usefully investigate specific patient conditions based on the uptake of specific radionuclide markers.

Within a nuclear medicine department, a high level of skill is needed to maintain camera systems that function optimally. This includes the implementation of specific calibration checks using special image phantoms to ensure image uniformity and prevent image artefacts. This high level of skill will also include a sound understanding of the physics of relevant imaging technologies such as single photon emission computed tomography (SPECT) and SPECT/CT, and positron emission tomography (PET) and PET/CT. In the past few years, SPECT/MRI has developed into an imaging modality, although it remains essentially a research tool.

Three specific themes are included in this paper. The first relates to the basics of conventional gamma cameras, where references are made to the core elements of photomultiplier tubes, an energy discrimination window, collimators, and sodium iodide crystals. SPECT/CT application examples are provided. These include spinal, cardiac, and cancer investigations. The SPECT/CT modality provides the ability, for example, to relate "hot spots" of activity to precise anatomical locations. Such information, for example, has the potential to make subsequent surgical interventions more successful. The second theme relates to the development and potential of PET/CT. Reference is made to the development of a "Time of Flight" system where the relative times of two photons detection event can potentially be calculated. The third theme is a comparison of SPECT/CT and PET/CT systems, with PET/CT having a significant advantage in terms of detected events when compared to SPECT/CT. This allows for better scan statistics with a larger number of detected events, as well as the ability to perform scans in shorter time periods. It is recognised that PET/CT can play a role in patient diagnosis when sites of infection are difficult to identify using CT/MRI, or SPECT/CT imaging technologies.

In contrast, by comparing nuclear medicine imaging technologies such as SPECT/CT and PET/CT, it is important to note that both of these technologies are developing, as if in parallel, and are demonstrating significant improvements in performance over a relatively short period of time. Reference is also made to the integration of MRI into SPECT and PET imaging. In the context of SPECT/MRI, there remains a key issue relating to the shielding of photomultiplier tubes in high magnetic fields for SPECT/MRI systems. In PET/MRI systems, however, modern semiconductors are essentially immune to high static magnetic fields. In general, however, MRI imaging takes significantly longer than CT imaging and so would restrict patient scan throughput.

Within the paper, key references to techniques and technologies are illustrated using images from published and reviewed journal papers. This has been found to be useful in identifying the core clinical set of applications that make use of nuclear medicine imaging technology.

2. Single photon emission computed tomography and SPECT/CT systems

2.1. Principle of SPECT imaging

The core of imaging technology within a nuclear medicine department relates to the detection of gamma ray photons from radioisotopes which decay within the tissue of the patient being scanned. In the earliest detection systems, a single detection device was moved across the site of interest (Blahd, 1996). This approach; however, was both slow and inflexible. The development of the gamma camera detection system provided to improve the image quality; nevertheless, the transition from rectilinear scanner systems to gamma camera technology was very slow. The conventional gamma camera image does not provide information about the relative distribution of radiation within the volume of the

patient. Fig. 1 indicates the basic elements of the original gamma camera where the initial gamma radiation passes through a collimator to absorb non-relevant photons. The basics of this design; however, are still replicated in even the designs of current state of the art gamma camera systems. Gamma rays passing through the collimator to be detected in the scintillation crystal. It is fabricated from sodium iodide material which is typically 6 to 12 mm thick. Light guides couple light from the upper surface of the scintillation crystal to the array of photomultiplier tubes. The crystal requires to be hermetically sealed to prevent the crystal material absorbing water vapour from the atmosphere. In addition, the lower surface of the scintillator crystal is lined with reflective material to increase the level of light detected by the photomultiplier tubes (Kharfi, 2013, Gramuglia et al., 2021).

In the photomultiplier devices, incoming photons of light eject electrons from the photocathode layer as indicated in Fig. 2. Initially these electrons are attracted to the first dynode where a multiplication of electrons takes place and which is repeated between the dynodes that resulting in a voltage pulse at the output of the device.

Fig. 3 indicates the types of collimator which can be used for conventional image capture. The use of diverging, converging and parallel hole collimators; however, reduces the potential number of photons to reach the detecting crystal.

Pinhole collimators as indicated in Fig. 3 utilise simple geometrical optics, for example to magnify the image size of small organs such as the heart and thyroid. The parallel plate collimator is the most widely used collimator for use with conventional gamma camera systems and where the object plane size is replicated in the image plane without inversion. In the diverging collimator the channels of the collimator converge to a point some distance behind the image plane, resulting in a non-inverted image of reduced size. In the converging collimator, the channels of the collimator converge to a point some distance behind the object, resulting in a non-inverted image of increased size. The collimator; therefore, has a key role in scaling the size of detected images. It is important in state of the art imaging systems involving SPECT/CT and PET/CT that there is complete registration between the images captured within independent imaging technologies.

Such direct planar imaging technology can image specific regions of interest or be used in whole body imaging to create bone scans as indicated in Fig. 4.

This level of image quality provides specific clinical information that can be benefit for patient diagnosis and treatment. There is; however, a low level of confidence relating areas of increased radioisotope activity with specific anatomical features.

2.2. Factors influencing image quality

A number of factors have been identified which determine the intrinsic spatial resolution of a gamma camera system. One factor relates to Compton scattering of the incident gamma ray photon where information of the initial trajectory of the incident photon is degraded. Another key factor influencing spatial resolution is the inherent statistical fluctuation in the number of photons detected by the photomultiplier tubes from each scintillation event. In addition, as gamma photon energies reduce, then the level of statistical fluctuations in the number of light photons

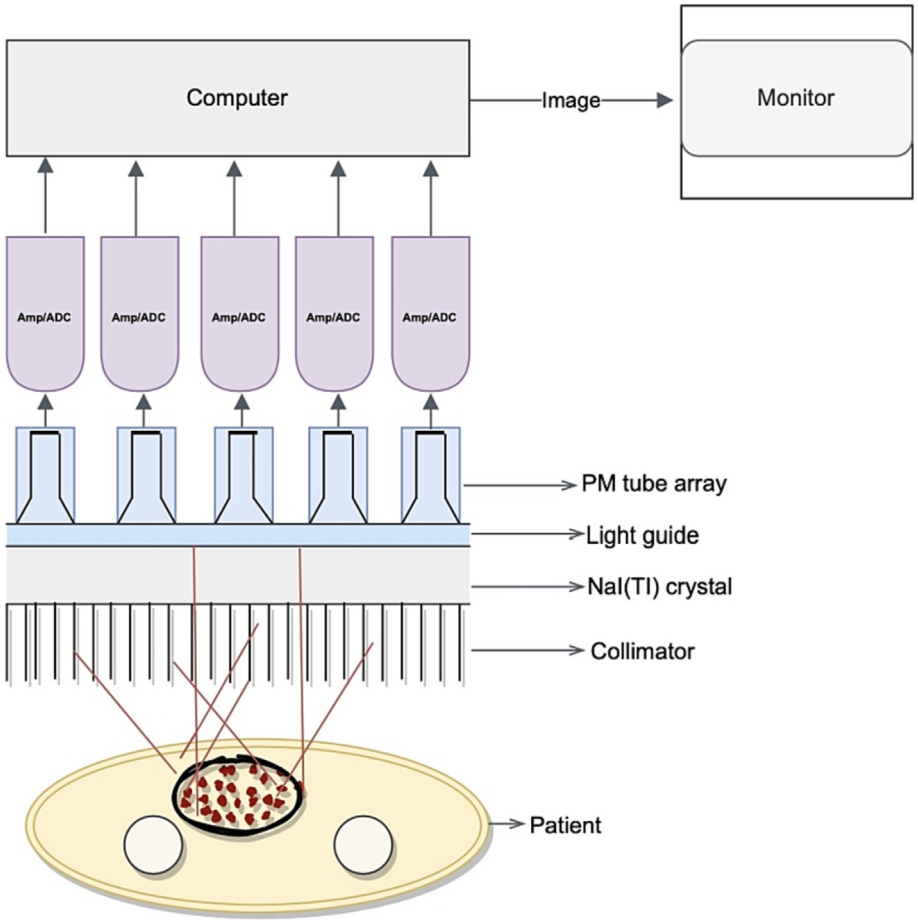

Fig. 1. Basic principles and components of a modern gamma camera.

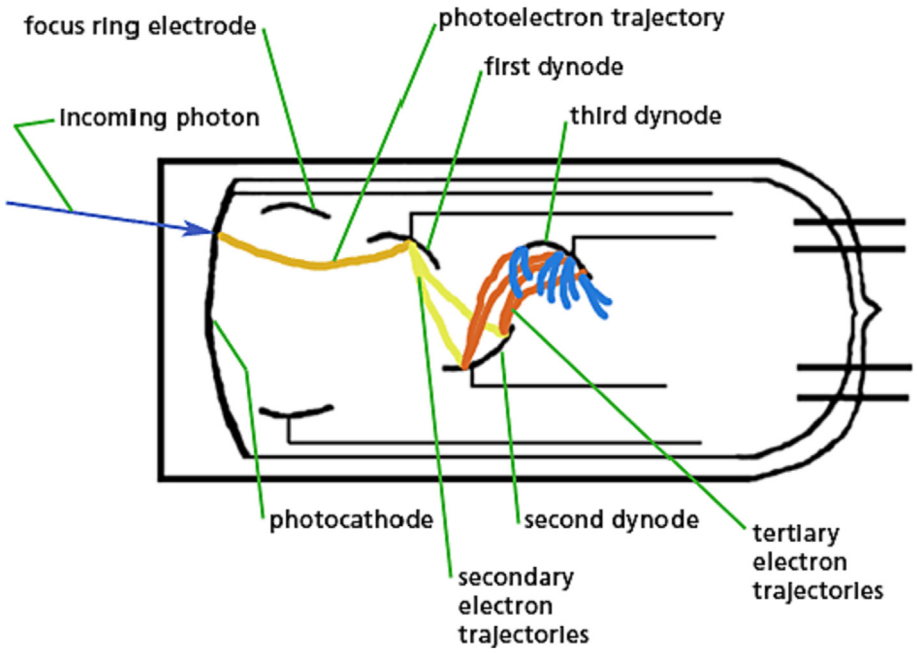

Fig. 2. Basics of photomultiplier tube function – where incident light photons eject electrons from the photocathode surface where a multiplying cascade of electrons takes place across the stages of the device. (Piccard, 2005).

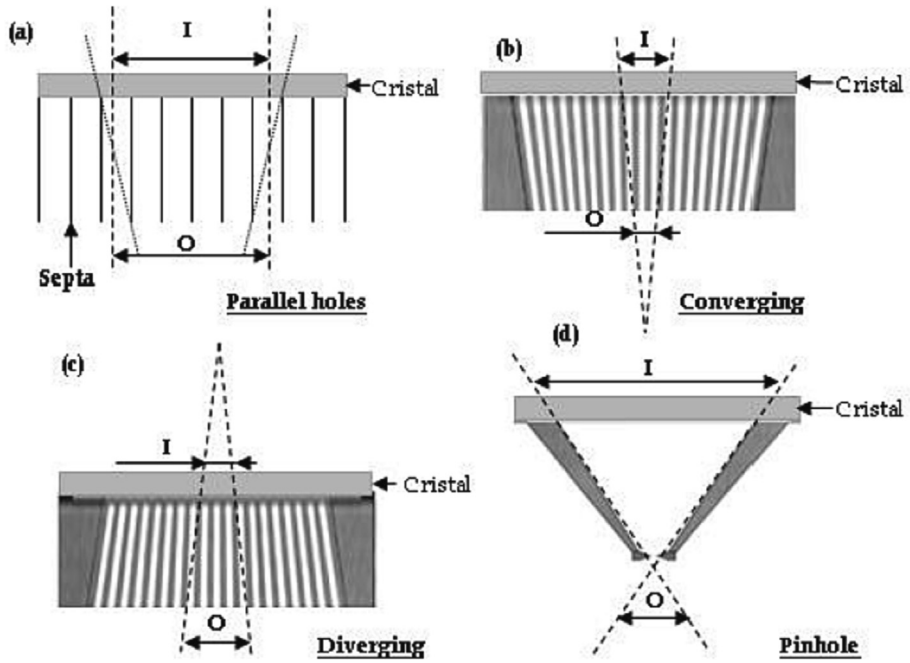

Fig. 3. Basic types of collimator use in conventional gamma camera (O: object, I: Image) (Kharfi, 2013).

released within the detection crystal also increases (Cherry et al., 2012).

Increasing the thickness of the scintillation crystal increases both the chance of Compton scattering and the level of statistical fluctuation in light detected by the photomultiplier tubes.

With increasing gamma ray energy; however, the photo peak detection efficiency decreases (Fig. 5) so a compromise is required between overall detection efficiency intrinsic spatial resolutions (Cherry et al., 2012).

Energy resolution is also a consideration for image quality, where the ability to reject photons of reduced energy which has experienced Compton scattering will improve overall image quality. For ^{99m}Tc, for example, a typically selected energy window of between 130 keV and 150 keV is selected.

2.3. Most common radionuclides used in SPECT nuclear medicine applications

Table 1 summarises radionuclides most frequently used for imaging applications in SPECT nuclear medicine.

The emission of low energy photons from ^{99m}Tc which are not completely absorbed by the body help to reduce the radiation dose

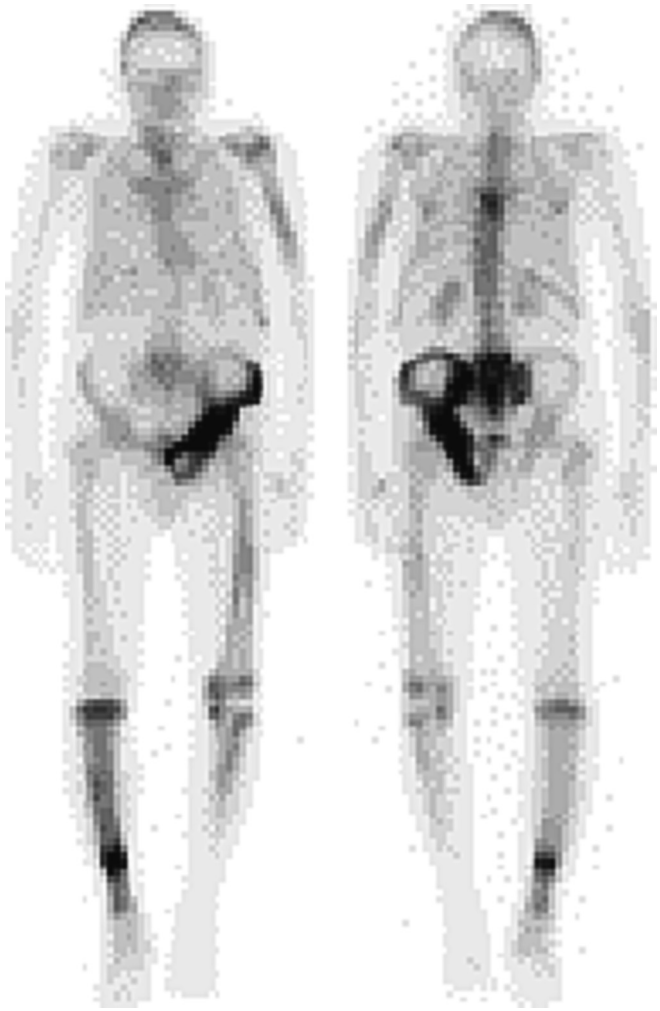

Fig. 4. Whole body scan using 99mTechnetium-methylene diphosphonate (99mTc-MDP) showing involvement of Paget's disease (Cook, 2010).

absorbed by the patient with administration of the radioisotope. In addition, ^{99m}Tc can be combined with biologically active compounds to track physiological activity within the body. The use of ^{201}Tl in cardiac imaging dates back to McKillop in the 1980′s where it was the first radioisotope to be used for this application (McKillop, 1980). ^{67}Ga can be attached to specific compounds for preferential take up at sites of acute and chronic infection where Gallium 67 is particularly useful in imaging osteomyelitis that does not involve the spine. ^{111}In can be labelled with platelets to identify the location of thrombus and can also be attached to peptides and proteins to identify certain rare forms of cancer.^{133}Xe is used in the gas form for respiratory studies and as gas in liquid solution for cerebral blood flow (Cherry et al., 2012; Appelgren, 2020).

2.4. SPECT and SPECT/CT imaging

Details of radioisotope distribution within tissue volumes can be obtained with the use of SPECT where the gamma camera head is rotated around the patient in a mode similar to CT using X–rays and where a reconstruction of radioisotope image capture data is undertaken. In some applications, SPECT images can be achieved by a single 360-degree rotational scan. This technology is now routinely integrated with CT to provide SPECT/CT imaging where the CT information provides a reference framework of anatomical information to improve the diagnostic value of the SPECT image data. SPECT images are typically created based on a matrix of 64x64 or 128x128 pixels within small fields of view such as in heart studies. Single head camera can be rotated around the patient to capture a SPECT image, while dual headed cameras are also employed where each camera independently acquires data from its own field of view. Gamma cameras can be configured through body contouring mode to remain as close as possible to the region of the body being imaged; such as in cardiac studies in order to optimise scan quality. While early SPECT systems utilised "image fusion technology" of CT images taken from separate imaging systems, current SPECT/CT systems with inbuilt CT systems allow automatic fusion of images and with appropriate tomographic correction based on body mass detected in CT mode. There is also an advantage in the footprint of scanning systems to pro-

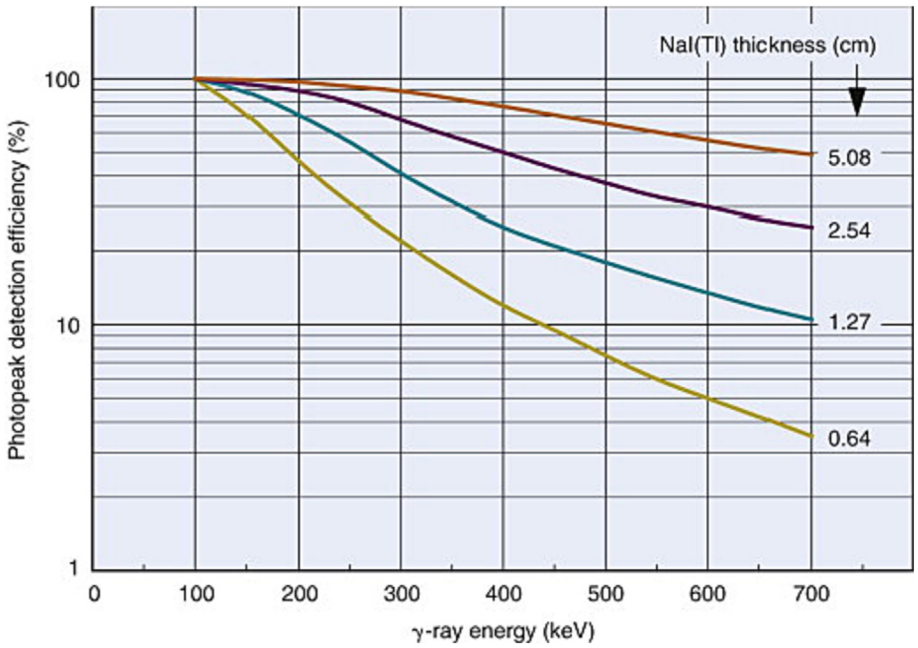

Fig. 5. Variation of photo peak detection efficiency with gamma ray energy for Na (Tl) detectors (Cherry et al., 2012).

duce radioisotopes and CT imaging undertaken in the one integrated system such as the Philips BrightView SPECT/CT system as indicated in Fig. 6.

2.5. SPECT/CT applications

2.5.1. Bone imaging

Fig. 7 shows a typical SPECT/CT image where the scan is assessing the uptake of a radioactive nuclide within the spinal column. The annotated regions in the right image of the spinal column are indicated regions of interest. SPECT images provide therefore a new dimension in radioisotope diagnostic imaging where the matrix of radioactivity activity is closely referenced to the anatomical framework provided by the CT image. In many systems, SPECT and CT image capture take place at the same time.

Fig. 8 indicates the usefulness of fused SPECT and CT images to identify areas of increased radioisotope uptake and where increased activity was identified with degenerative bone conditions rather than bone metastases. The radionuclide that used was 99mTechnetium-methylene diphosphonate ^{99m}Tc-MDP.

Table 1
Indication of radionuclides with potential imaging application in SPECT Nuclear Medicine applications.

Radioisotope	Decay Mode	Energy emission	Half Life (Hour/Day)
^{99m}Tc	Isomeric transition	140 keV	6.03 h
^{201}Tl	Electron capture	68–80 keV × rays	3.05 d
^{67}Ga	Electron capture	93, 185, 300 keV	3.26 d
^{111}In	Electron capture	171, 245 keV	2.8 d
^{123}I	Electron capture	159 keV	13.2 h
^{133}Xe	Beta emission	81 keV	5.25 d

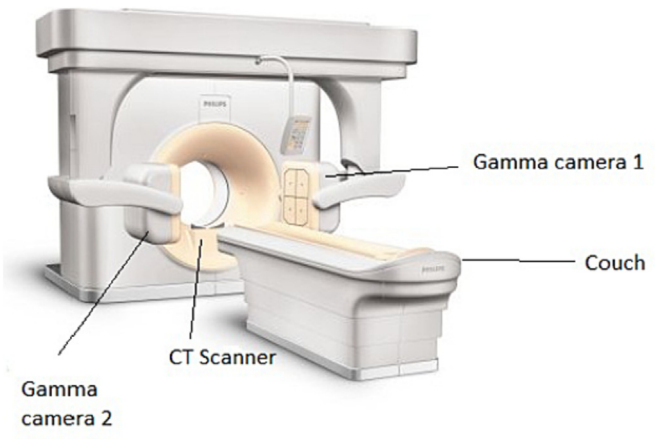

Fig. 6. Philips BrightView SPECT/CT system. (Courtesy Philips Medical).

2.5.2. Myocardial perfusion imaging

Increasingly SPECT/CT is becoming a reference diagnostic tool for identification of heart disease where arterial stenosis can be identified with high precision using CT facility and associated ischemic regions within each arterial branch can be readily identified using SPECT. This SPECT technique is described as myocardial perfusion imaging (MPI). In Fig. 9 (right image) the white arrow indicates a region of 99 % stenosis (indicated by CT) and the black arrows indicate a region of reduced perfusion (indicated by SPECT) (Jinzaki et al., 2011).

Fig. 10 indicates the scan of an 84 years old male patient with a history of congestive heart failure, hypertension, coronary artery disease and myocardial infarct as captured by a Philips BrightView SPECT/CT system (Philips, 2010).

A previous study shows that SPECT/CT appears to offer superior diagnostic and reference information to identify heart defects rather than fusion of data from separate systems (Gaemperli et al., 2011). In addition, another study identifies the phase of rapid technological change in the context of cardiac imaging and identifies the emerging trend for SPECT/CT and PET/CT to take a dominant role in such developments (Flotats et al., 2011). It is also indicated that on-going studies are likely to confirm such trends (Hachamovitch et al., 2009).

2.5.3. ^{131}I thyroid Scan:

Diagnostic ^{131}I SPECT and SPECT/CT imaging.

The natural uptake of the thyroid for iodine as ^{131}I provides a useful means of monitoring function of this organ (Avram, 2012). Fig. 11 indicates the use of SPECT/CT function to identify status of regions of increased ^{131}I uptake and this example indicates no evidence of tumour extension beyond the original margins. The fused SPECT image with CT scan image allows improved identification of anatomy identified with increased radioisotope take up.

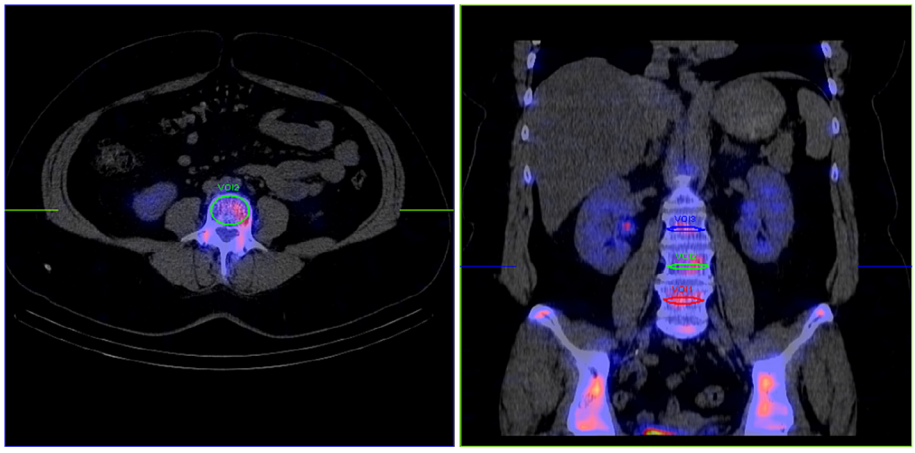

Fig. 7. SPECT/CT image of fused sets of data (transverse and coronal) where the scan is assessing the uptake of 99mTechnetium-dicarboxypropane diphosphonate (^{99m}Tc-DPD) within the spinal column (Cachovan et al., 2013).

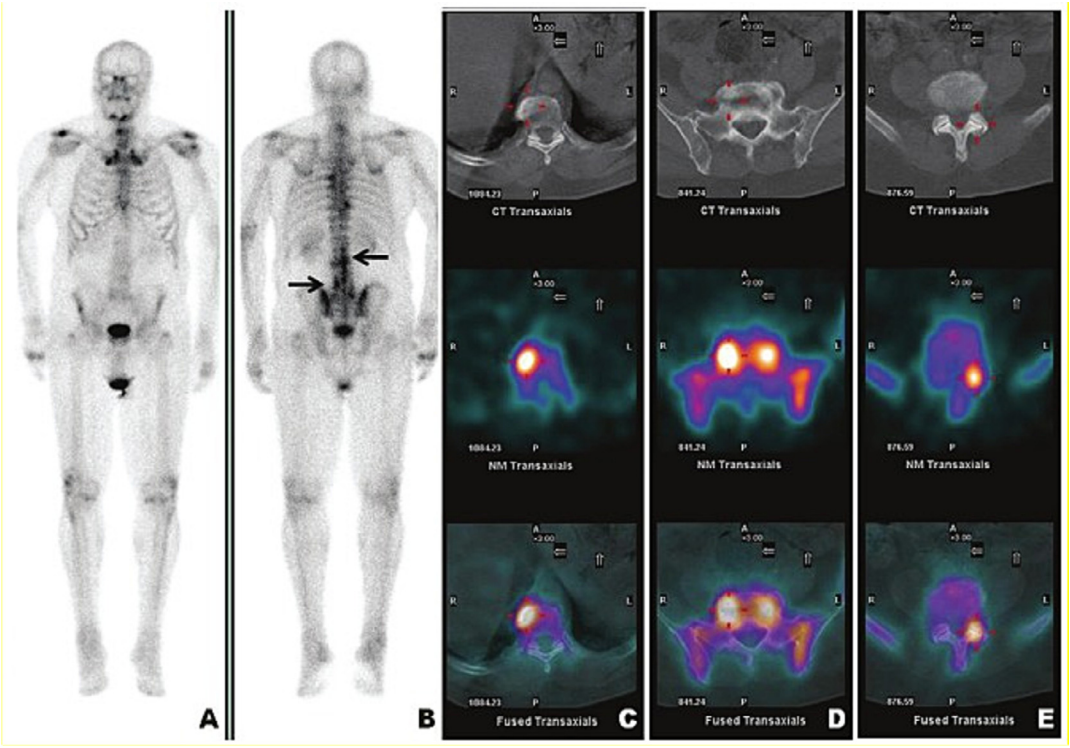

Fig. 8. Image A/B: Planar whole body scan images. Images C/D and E indicate separate CT, SPECT and fused SPECT/CT images of selected anatomical spinal areas (Bhargava et al., 2012).

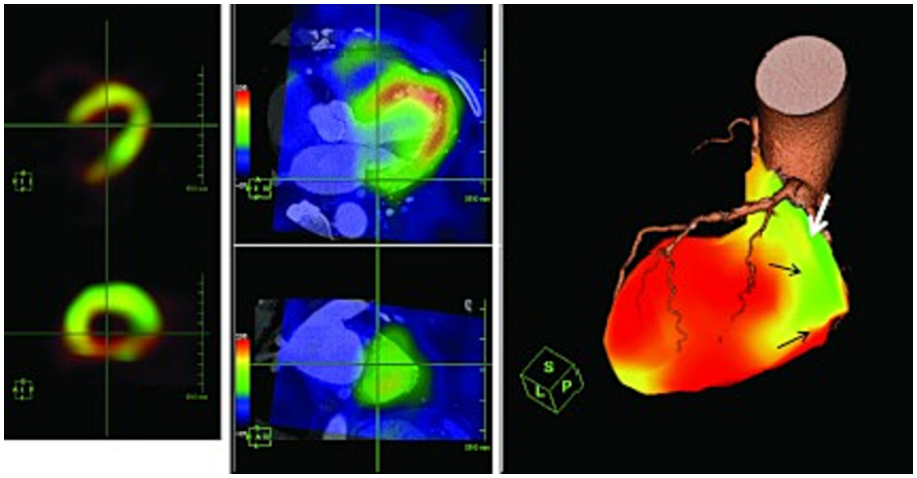

Fig. 9. Right Image: The white arrow indicates a region of 99% stenosis (CT scan) and black arrows an area of reduced perfusion as highlighted from SPECT image (Jinzaki et al., 2011).

3. Positron emission tomography (PET) and PET/CT systems

3.1. Principle of PET imaging

The principle of PET imaging is indicated in Fig. 12 where a positron is released by the radioisotope as part of the process of positive beta decay. The positron loses energy as part of interactions in tissue and after the positron has travelled a short distance (typically around 1 mm), the positron will decay into two gamma ray photons where each one has energy of 511 keV. As a result, with no subsequent interactions experienced by the photons, these photons will track in equal and opposite directions. However, it is possible for either photon (or both) to experience some degree of Compton scattering; so that the 180-degree is modified slightly. In addition, there may be residual momentum associated with the positron before it decays and which is reflected in the net momentum of the radiated gamma ray photons. However, the angular deviation between photons will be typically less than 0.25 of a degree (Cherry et al., 2012).

3.2. Coincidence events in PET

Coincidence events can be described as true events where the event arises from a valid coincidence event. As well as this, it can be as background events where some degree of photon scattering is experienced or the event is based on random event detection

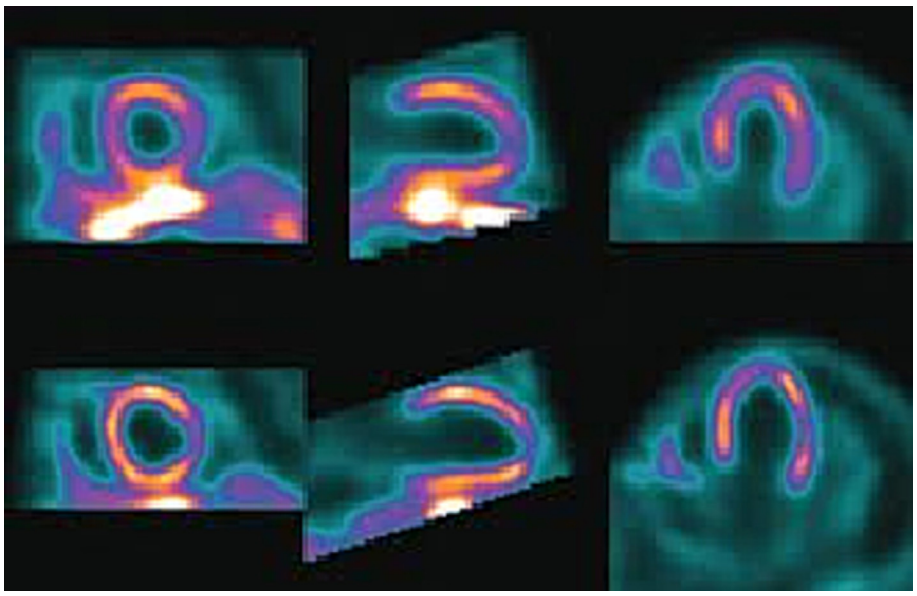

Fig. 10. Comparison of 64 × 64 matrix (top) with 128 × 128 matrix (bottom) for Philips BrightView SPECT/CT system for a patient with a history of congestive heart failure, hypertension, coronary artery disease and myocardial infarct (Philips, 2010).

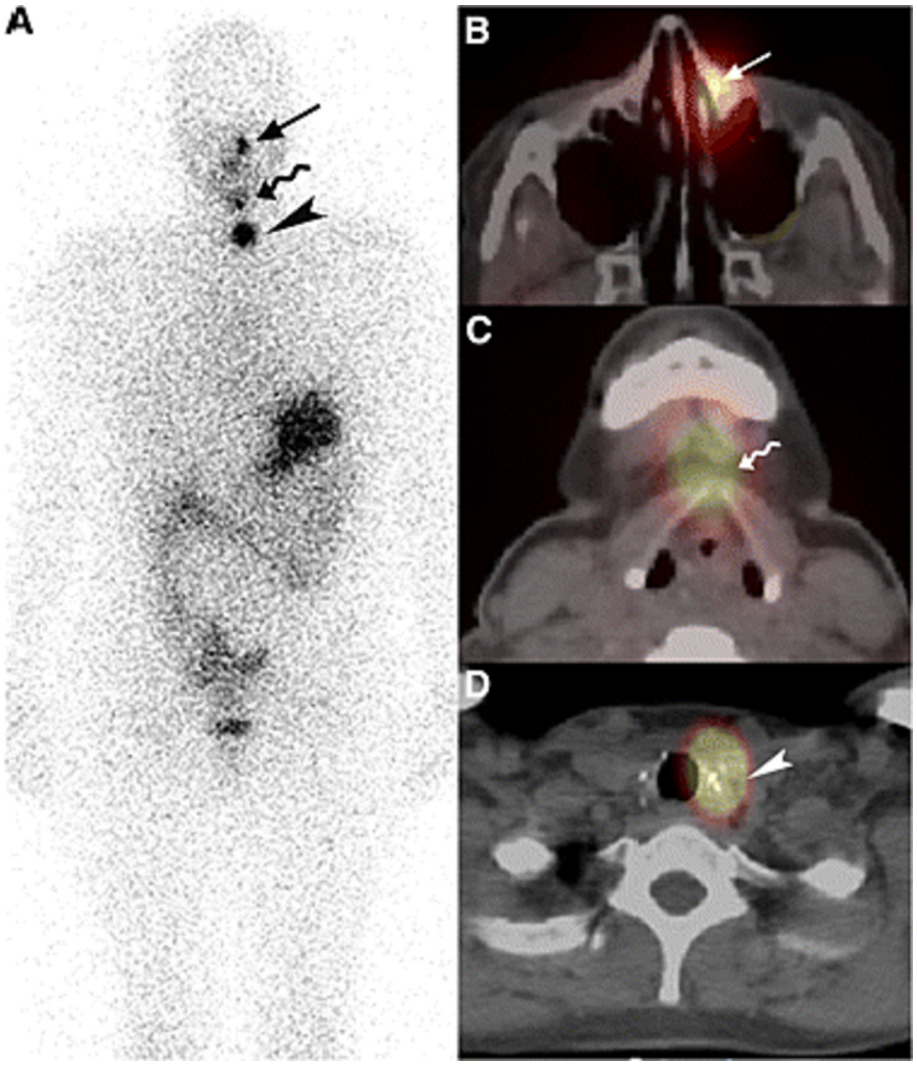

Fig. 11. Image A: Planar whole body image indicates three centres of potential activity. Image B: SPECT/CT image indicates benign involvement of nasolacrimal duct; Image C: Indication of benign embryologic migration of thyroid. Image D: Indicates tumour that remnant post-surgery (Avram, 2012).

where; for example, two separated positron emissions produce detections events where only one photon from each event is detected by the system and where one of the photon pairs is absorbed in the patient tissue. These states of detection are indicated in Fig. 13. In the middle example, the coincidence event arises when two independent positrons decays result in only two photons being detected by the detector ring. The process of event detection is also termed annihilation coincidence detection (ACD) (Shukla and Kumar, 2006).

Within the process of image analysis, a key element is to identify the distribution of so-called line of response (LOR) of the coincidence events. Where in practice, the LOR has a limited width, as the emitted photons are not exactly 180 degrees apart. The photon energies of the CT scan component are typically in the range 100–140 keV, which requires the CT attenuation map to be scaled up to that of 511 keV in order to correct PET images for tissue absorption. This tends to be undertaken within specific LOR trajectories. Therefore, it is relevant to consider that image reconstruction based on technique of TOF method. For detection at the level of 1 mm, time resolution at the level of picoseconds (ps) is required (Cherry et al., 2012; University of Virginia, 2012).

Most detector systems, however, would have detection times of several hundred picoseconds, indicating that measurement resolution less than 1 cm is not possible with TOF technology. Moses identifies that while time of flight PET is not widely utilised in current commercially available systems, there remains potential for improvement with on-going developments in scintillators, photodetectors, and high-speed electronics (Moses, 2007). Additionally, the potential advantages of TOF mode are more recently described to include shorter scan times and improved image quality (Conti, 2011). Performance factors for specific PET scintillators are indicated in Table 2.

Table 2 would suggest that Lutetium oxyorthosilicate (LSO) scintillator material would be more appropriate for TOF image re-construction algorithms.

The detection system looks for two events within a coincidence time window specific to the detection technology utilised. The value of this coincidence window is typically in range from 4 to 12 ns. Where an element of collimation is applied within the detection ring and which restricts the range of coincidence events detected, then the reconstruction mode is termed two-dimensional (2D). Where collimation is essentially not used, the image reconstruction mode is described as three-dimensional (3 D) and requires more complex algorithmic image reconstruction processes (Cherry, 2012).

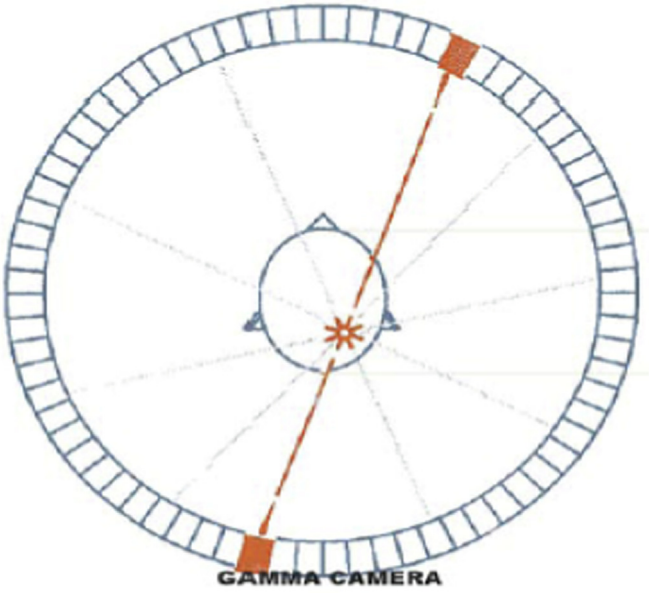

Fig. 12. Principle of PET imaging.

3.3. Most common radionuclides used in PET nuclear medicine applications

Table 3 indicates the set of radionuclides potentially available for PET/CT studies.

^{18}F is generated from cyclotron irradiation of water enriched with ^{18}O. ^{13}N is created by irradiating^{16} O water atoms by 16.5 MeV protons. Cardiac imaging can also be undertaken with the use of ^{82}Rb and where ^{82} Rb is rapidly absorbed by heart tissue. In addition, ^{82}Rb, with a half life of 1.27 min, is produced by means of a generator rather than a dedicated cyclotron source.

One consideration for image quality is the distance positrons are likely to travel in matter before they revert to two gamma rays. Table 4 indicates the relative performance of PET radionuclides.

A key requirement for PET imaging is that the radionuclide is transferred to a molecule that will be absorbed in the target scan volume. Fluorodeoxyglucose (FDG) or 2-deoxy-2-(^{18}F) fluoro-D-glucose is a compound which is created where ^{18}F replaces groups within a glucose molecule. The FDG molecule, however, is small and able to cross the blood brain barrier and in its metabolic activity closely resembles the characteristics of glucose. The^{11} C radioisotope can be readily attached to small organism visa replacement of C atoms, thus giving rise to a broad range of imaging tracers. In addition, use is being made of ^{18}F FDOPA for identification of brain tumours whose structure is indicated in Fig. 14.

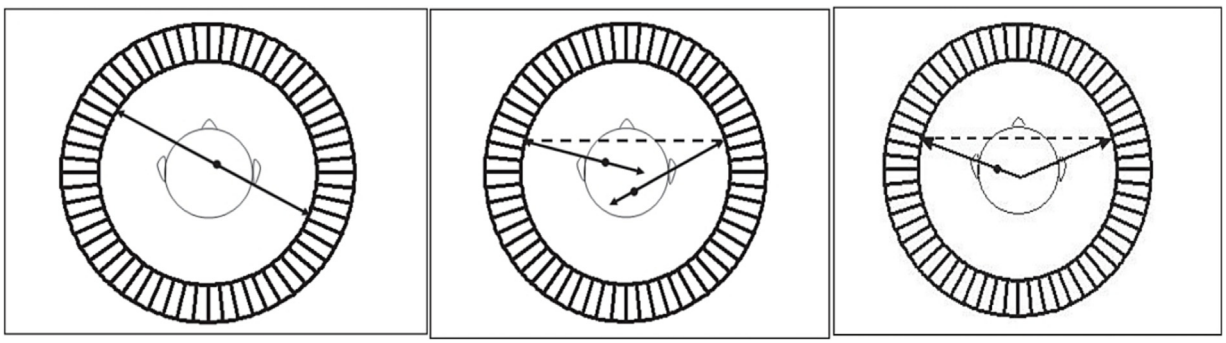

Fig. 13. (left) True coincidence event: (centre) accidental or random coincidence event; (right) misposition of coincidence event (Shukla and Kumar, 2006).

Table 2
Characteristics of PET scintillators.

Characteristic/parameter	Bismuth germanate (BGO)	Lutetium oxyorthosilicate (LSO)	Sodium iodide NaI (Tl)
Crystal Density (gm/cc)	7.13	7.40	3.67
Eff. Atomic Number (Z eff.)	74	66	51
Decay Time (nano *sec.*)	300	40	230
Light output	15	75	100
Refractive Index	2.15	1.82	1.85

Table 3
Summary of radionuclides used in PET/CT studies.

Isotope	Half life (minutes)	Production mode
^{18}F	110	Cyclotron
^{11}C	20	Cyclotron
^{13}N	10	Cyclotron
^{15}O	2	Cyclotron
^{68}Ga	68.3	Generator
^{82} Rb	1.27	Generator

Table 4
Range and energy of positrons emitted by major positron emitting radionuclides.

Radionuclide	Maximum energy (MeV)	Maximum range in the tissue (mm)
^{18}F	0.63	2.6
^{15}O	1.74	8.4
^{13}N	1.20	5.4
^{11}C	0.96	4.2

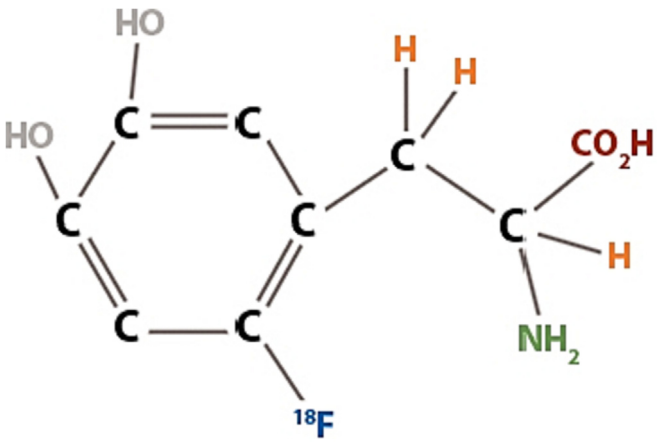

Fig. 14. Structure of ^{18}F FDOPA that is uses for detection of brain tumours.

3.4. PET and PET/CT imaging

In PET imaging, use is made of the coincident emission of two photons from the decay of radioactive isotopes such as^{18}F. In this process of positron emission, the gamma ray photons carry equal and opposite levels of momentum from the decay and the detection system can compute the co-ordinate of origin of the photons by measurement of the relative TOF of the two particles. As the PET scanning system is rotated round the patient, details of radioisotope concentration within a slice of tissue can be computed.

The inclusion of CT scanning using X-ray beam technology has been incorporated into PET imaging to produce PET-CT imaging where the imaging modalities are combined to improve the diagnostic usefulness of the separate modalities. Therefore, for example, regions of interest that highlighted by radioisotope imaging can be more closely related to patient anatomy. There is a preference for systems which provide PET/CT within a single scanning facility rather than separate PET and CT systems where images are fused from essentially different imaging systems. A key element of the software of such systems is the software function which fuses the two imaging data together. In addition, the data of the CT scan provides key information to provide image correction for tissue absorption of radionuclide detection data. An example of this fusion or image systems is indicated in Fig. 15, where the PET image shows the extent of progression of right nasopharyngeal carcinoma and which would allow improved management of the patient condition either through radiotherapy or surgery (Varoquaux et al., 2013).

3.5. PET/CT applications

3.5.1. Lung cancer scanning

PET/CT is used routinely to identify sites of lung cancer, where the functional activity is identified with^{18} F FDG uptake and the precise location and size of the lesion is confirmed with the CT scan. Fig. 16 indicates the routine use of PET/CT for diagnosis of lung cancer.

3.5.2. Brain imaging

L-DOPA is a drug used in the treatment and investigation of Parkinson's disease where its action increases concentrations of dopamine on a short-term basis. Fluorodopa (F-DOPA) is created where radioactive ^{18}F is inserted within the molecule as shown in Fig. 17. F-DOPA is selectively taken up by neuro endocrine tumours and consequently allows PET/CT to image such structures (Jora et al., 2011).

Jora et al. study describes the use of a range of PET radionuclide traces for diagnosis of a range of 23 patients (8 preoperative and 15 postoperative) for primary brain tumours. It was identified that 18F-FDG provided better correlation to identify tumour grade than 18F-FDOPA. Moreover, ^{18}F-FDG PET imaging can be used to diagnose Alzheimer's disease (Chételat et al., 2020) and as shows in Fig. 18 (Johnson et al., 2012).

Radioactive tracers are also playing a significant part in research into disease progression of Alzheimer's disease where specialist tracers such as C-Pittsburgh compound B (PIB) and FDDNP in addition to^{18}F FDG are able to detect different aspects of disease progression/control in association with specific drug treatments (Wang et al., 2022). The radionuclides are in effect sensitive to specific levels of metabolic activity. This indicates the value of PET imaging as both a diagnostic tool and as a means of assessing a range of pharmaceutical interventions.

3.5.3. Cardiac PET/CT

A range of radionuclides are available for undertaking PET/CT cardiac studies and where a key parameter being investigated is the degree of perfusion of tissue at specific levels of exercise (see Fig. 19)

Cardiac PET and cardiac PET/CT imaging has been undertaken using^{13}N since the earliest days of PET technology (Schelbert et al., 1982). Machac describes details of ^{13}N PET cardiac imaging. One advantage of the ^{13}N PET radionuclide is the low residual value of the momentum carried by the positron before it decays to the two gamma rays. This improves the overall image resolution. The ^{13}N radionuclide is present in the form of ammonia molecules (NH_3) which pass readily from the vascular pool into cardiac tissue

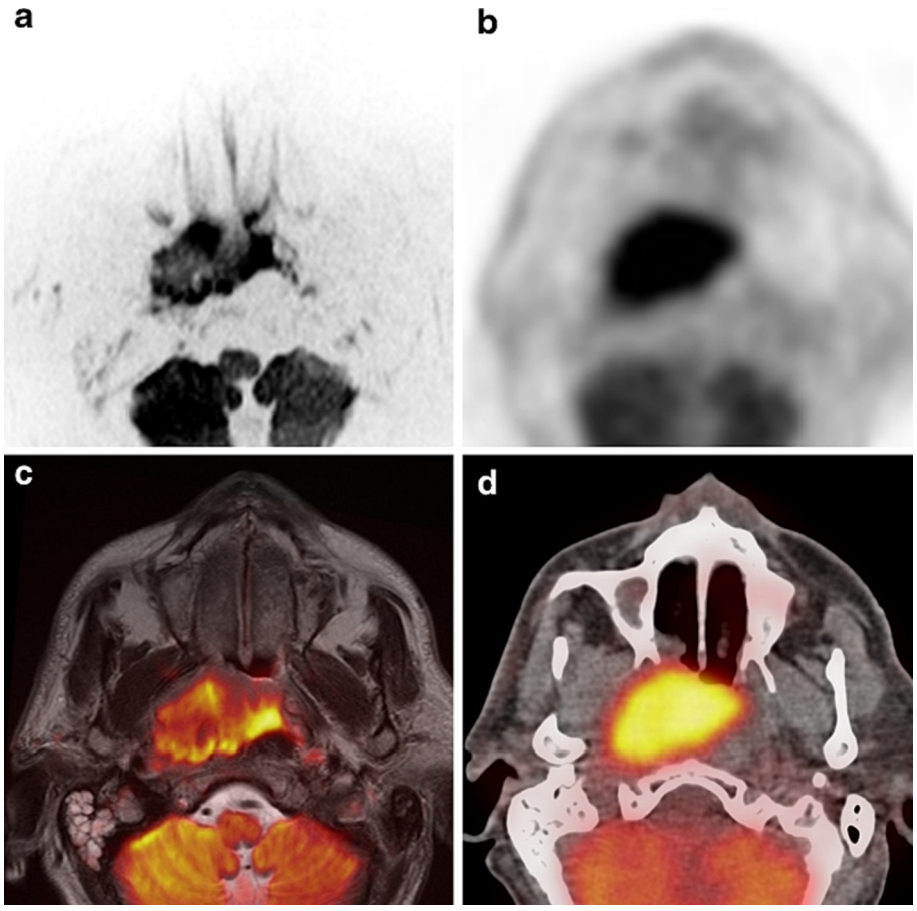

Fig. 15. Image (d) is the fused image of PET scan and CT image for identification of right nasopharyngeal carcinoma (Varoquaux et al., 2013).

(Machac, 2007). Fig. 20 indicates a specific investigation relating to ^{13}N.

Rubidium 82 has been in routine use in North America since the 1980′s as a radionuclide used for cardiac functional analysis. An expert review by Juarez-Orozco et al. describes Rubidium 82 constitutes the most used PET perfusion radiotracer in the USA (Juarez-Orozco et al., 2018). Within clinical investigation, a key parameter relates to identification of normal and abnormal clinical conditions such as the identification of the Transient ischemic dilation (TID) ratio. Fig. 21 indicates a series of scans to identify TID values for a range of patients with heart conditions and where comparison was made to TID values derived from SPECT images (Rischpler et al., 2012).

4. SPECT CT and PET CT Modalities: Comparisons

4.1. Introduction

Since the emergence of SPECT/CT and PET/CT as imaging modalities in nuclear medicine, there have been efforts to evaluate clinically the relative advantages of their techniques. Rahmim and Zaidi identify many of the areas of debate relating to the two technologies (Rahmim and Zaidi, 2008). One example is the relevance of the biological activity of the tracers of SPECT and PET and which is subsequently reviewed within analysis of SPECT/CT and PET/CT imaging in specific clinical investigations. Authors indicate that while the potential of dual tracer imaging has already been realised for SPECT/CT, the potential of this technique remains uncertain for PET/CT; however, more recent researchers indicate the value of ^{18}F-FDG and ^{11}C-acetate PET/CT in the diagnosis of renal angiomyolipoma (Rahmim and Zaidi 2008; Ho et al., 2012). Dual tracer imaging is easier to achieve in SPECT where it is typically possible to use appropriate different energies such as ^{99}mTc (140 keV) and ^{201}Tl (75 keV/167 keV). For PET; however, the gamma ray photons are the same energy. The authors also indicate that PET/CT techniques can apply superior attenuation algorithms to image reconstruction compared with SPECT/CT (Madsen, 2007). This contributes to higher diagnostic function of PET/CT imaging. It is relevant to indicate that while PET/CT and SPECT/CT have been compared as separate modalities, it may also be possible to combine the modalities (SPECT/PET/CT) in a single imaging system (Madsen, 2007). This system will aid as a key for early diagnosis and treatment for cancer, cardiac and neurological diseases, however, the body will receive high dose of radiation. Such systems are in fact now available but not widely taken up available (Madsen, 2007; Veit-Haibach et al., 2013).

4.2. PET/CT and SPECT/CT resolution

Both PET/CT and SPECT/CT systems are developing technologies to improve image resolution. Typical values of PET resolution are around 5–7 mm while those of SPECT are around 10–14 mm (Lodge et al., 2005). However, the resolution of PET is linked to the radionuclide used, due to the effect of the transmission distance of the positron before it releases the pair of gamma ray photons. With SPECT; for example, developments in collimator are expected to lead to a reduction by an order of magnitude in cardiac scan time and improve resolution from around 8 mm to 3–4 mm (Beekman and van der Have, 2007). Further improvements in resolution are anticipated with TOF technology in PET imaging with

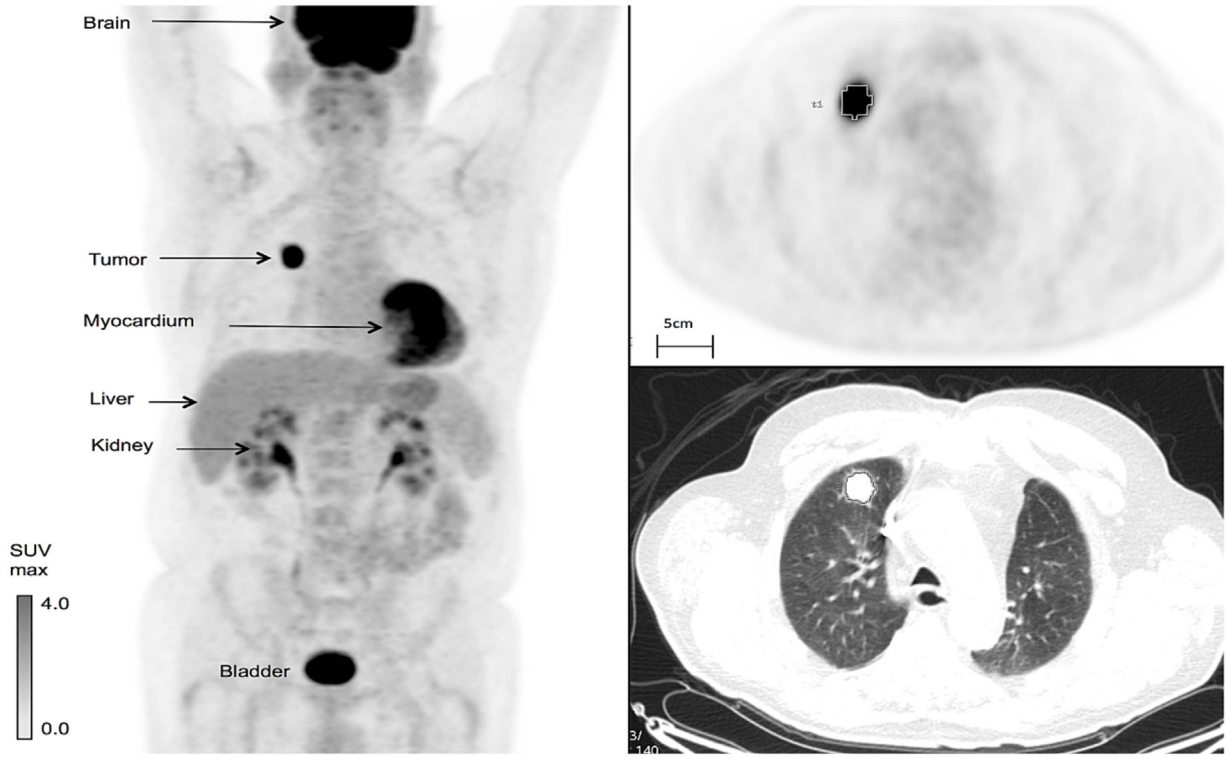

Fig. 16. Left: Whole body intensity projection ^{18}F FDG PET/CT. Upper right: PET Image tumour uptake Lower Right: CT image (Nair et al., 2013).

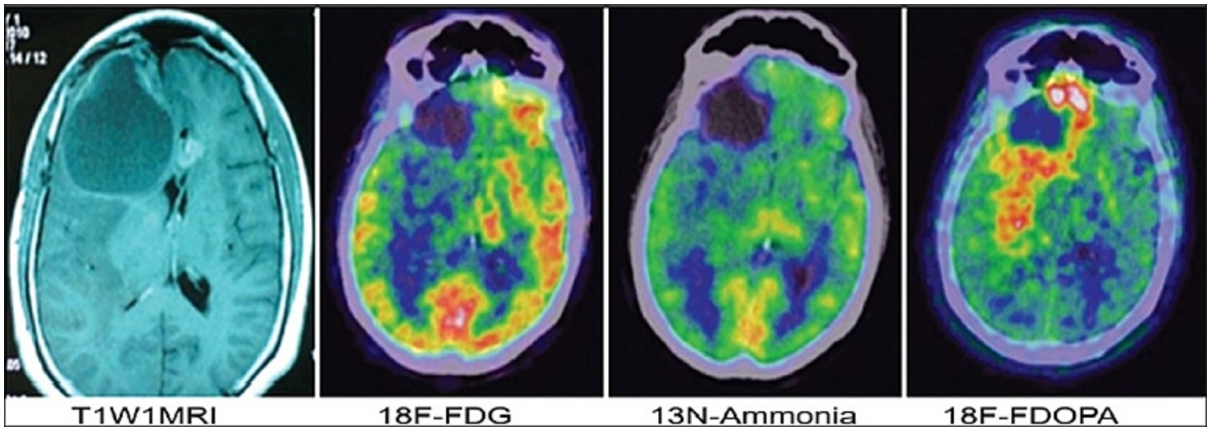

Fig. 17. Imaging of primary brain tumours using PET radionuclides (Jora et al., 2011).

development of faster responding scintillator materials and electronic circuits.

4.3. PET/CT and SPECT/CT sensitivity

One of the key differences between PET/CT and SPECT/CT is the significantly higher sensitivity of PET technology, where PET technology can detect in the region of two or three orders of magnitude more events than SPECT technology. One key contributing factor is the use of collimators with SPECT which while improving geometry of detection also remove a significant portion of incident radiation. This makes it possible to use PET/CT for obtaining multiple images from different fields of view and to complete individual scans more rapidly. While PET imaging is associated with rapid administration of radioisotope and prompt scanning, SPECT imaging has a key role for detecting long duration metabolic processes where metabolic processes may take several hours to become established. As a result, there are specific application areas for PET/CT and SPECT/CT which will remain non overlapping modalities based on different metabolic pathways (Crișan et al, 2022).

4.4. Specific clinical applications: SPECT/CT and PET/CT Comparisons

4.4.1. Myocardial perfusion imaging

Recent studies describe the advances in PET techniques for cardiac imaging and also highlight the problems of implementing advanced techniques using state of art imaging technologies (Di Carli et al., 2007; Dilsizian, 2021). PET radionuclides are identified as ^{82}Rb and ^{13}N-ammonia and where ^{82}Rb (half life 76 s) is available as a generator unit and ^{13}N-ammonia is produced from cyclotron systems. Uptake and distribution of ^{82}Rb, however, is strongly influenced by blood sugar levels of the patient, which can delay

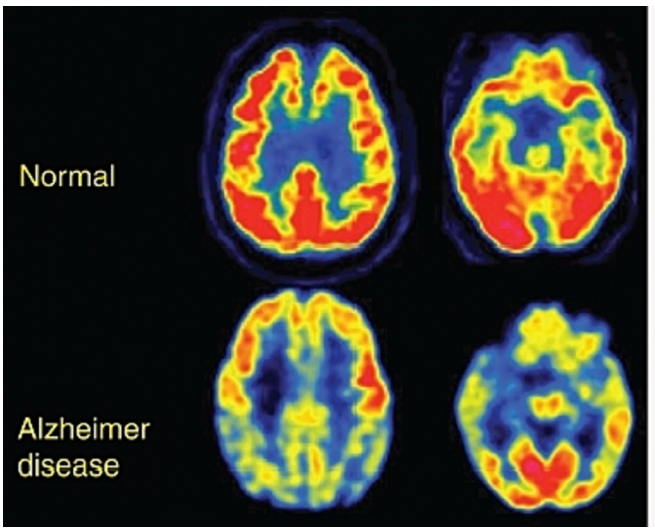

Fig. 18. Trans axial ^{18}F FDG-PET image of normal and patient with Alzheimer's disease. Where warm colours indicate normal metabolic activity and cool colours indicate reduced metabolic activity (Johnson et al., 2012).

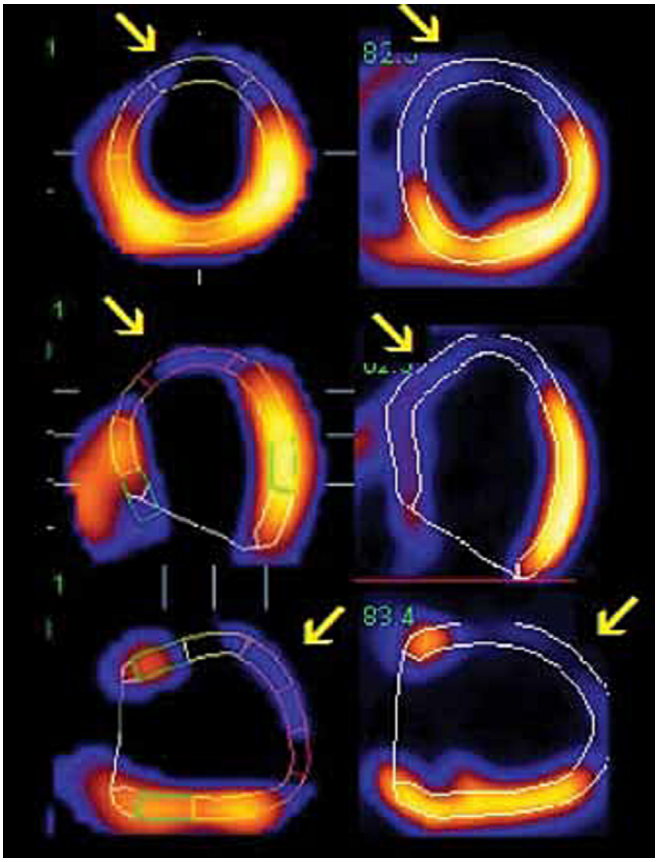

Fig. 19. Image shows the equivalence of 99mTc-MIBI perfusion (left) and ^{18}F FDG uptake (right) and where arrows indicate extensive perfusion defect (Kobylecka et al., 2012).

such testing. Evidence of the higher diagnostic value of PET is referenced in a number of early studies (Go, R.T et al., 1990; Stewart et al., 1991) and subsequently confirmed by a recent systematic reviewes (Al Moudi et al., 2011; Santos and Ferreira, 2019). It has been shown that myocardial perfusion PET/CT has high sensitivity and accuracy for detecting cardiac artery disease, including

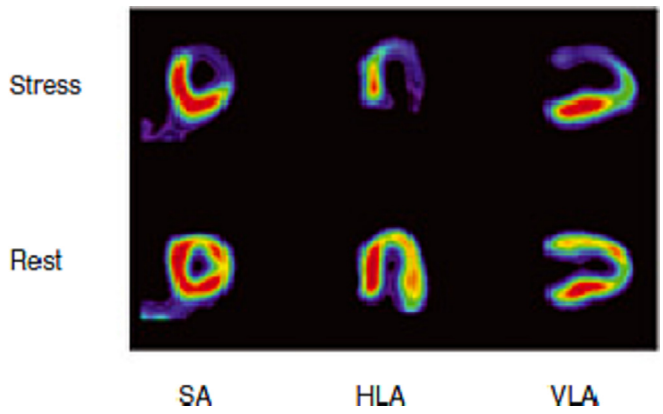

Fig. 20. Detail of ^{13}N cardiac imaging indicating anterior and lateral defects during induced pharmacological stress. SA, short axis; HLA, horizontal long axis; VLA vertical long axis (Machac, 2007).

women, and obese patients. Naya and Carli describe the usefulness of PET/CT imaging to quantify left ventricular function during peak stress and also to quantify levels of myocardial perfusion. The authors show that the combination of PET technique with the CT imaging data provide comprehensive scans of anatomy and function at a relatively low radiation dose (Naya and Di Carli, 2010). A review of role of SPECT/CT and PET/CT in myocardial perfusion imaging indicates that a significant advantage provided by PET / CT is the ability to provide accurate correction for tissue attenuation and which is reflected in provision of high levels of sensitivity and specificity identification of cardiac disease (Beller and Bergmann, 2004).

4.4.2. Whole body imaging

A key role of nuclear medicine imaging is whole body scanning for identification and localisation of primary and secondary lesions. A range of studies have been undertaken to assess the performance of whole body scintigraphy, SPECT/CT and PET/CT (Rager et al, 2018; Mosci et al, 2020; de Leiris et al, 2020). For example, Schirrmeister indicates the advantage of PET imaging for whole body image aimed at detection of bone metastases (Schirrmeister et al., 2001). The relative effectiveness of ^{131}I whole-body imaging, ^{131}I SPECT/CT, and ^{18}F-FDG PET/CT have been compared in the detection of spread of lesions from thyroid cancer (Oh, J.R et al., 2011). It was identified that while ^{131}I SPECT/CT, and ^{18}F-FDG PET/CT were both superior to ^{131}I whole-body imaging, ^{18}F-FDG PET/CT was superior to ^{131}I SPECT/CT in diagnosis of lesions associated with patients receiving multiple sequences of radioiodine therapy. However, there was no significant difference in diagnostic accuracy of bone metastases between whole body bone SPECT/CT (AUC 0.824 [0.74–0.90]) and PET/CT (AUC 0.829 [0.75–0.90], p = 0.41) as well as SPECT/CT does not provide additive diagnostic information over concomitant PET/CT (de Leiris et al, 2020).

Nuclear medicine imaging has also developed a role in the identification of conditions such as spondylodiskitis (inflammation of spinal disc space). A study evaluates the diagnostic value of whole-body PET/CT and bone scan combined with planar and SPECT/CT with ^{67}Ga (Fuster et al., 2012). It was identified that PET/CT provided the best diagnostic indication of spondylodiskitis. Where PET/CT gives fundamental information that may influence the treatment management of the disease. In addition, it was identified that the use of PET/CT as a general-purpose screening tool for the identification of abnormal sites of metabolic activity. Fig. 22, for example, identifies the image set of a patient where PET/CT was able to diagnose tuberculosis infection (Fuster et al., 2012).

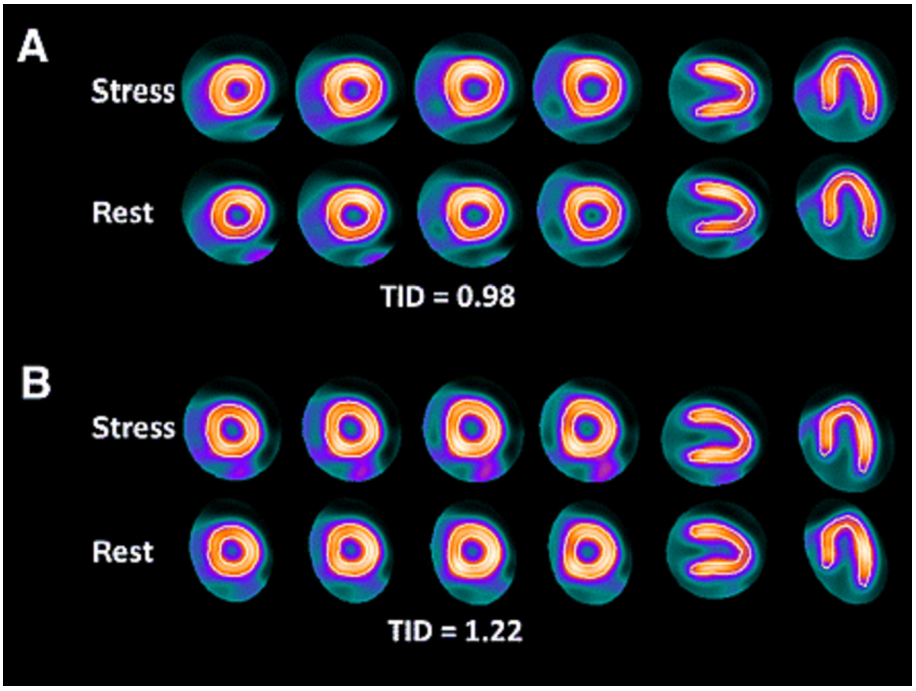

Fig. 21. Rubidium 82 scan Transient Ischemic Dilation Ratio (Rischpler et al., 2012).

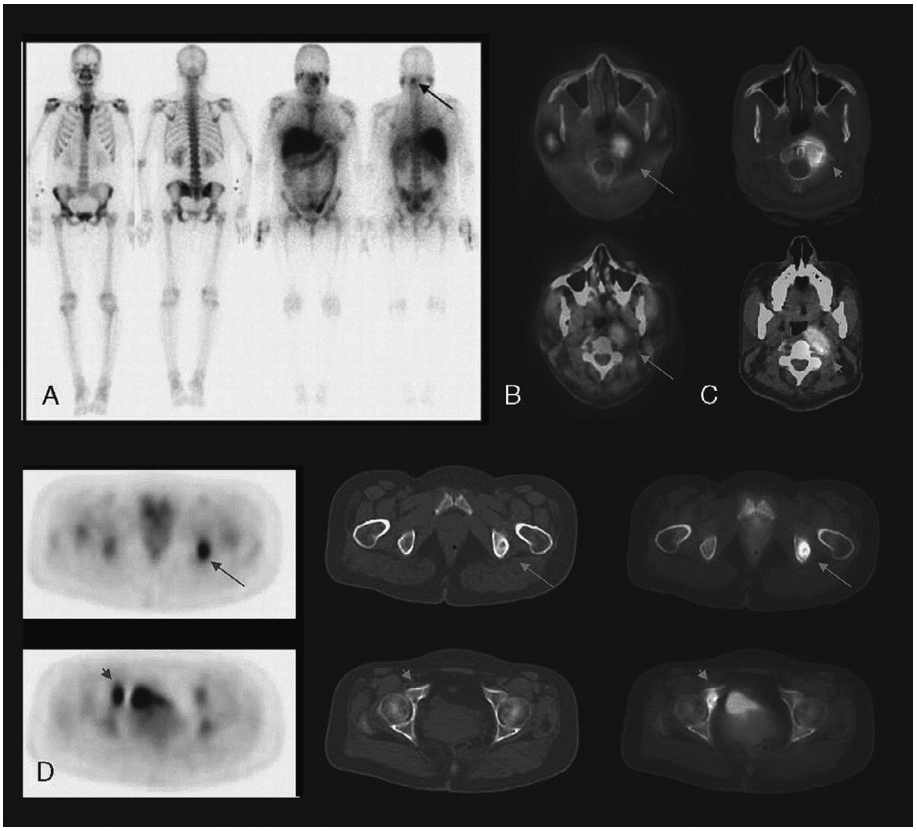

Fig. 22. Set of images in study for diagnosis of Spondylodiskitis in C1 and *C2* where planar images are indicated (A) and SPECT/CT ^{67}Ga scan images are indicated as (B) and PET/CT as (C) and (D) shows the adjacent soft tissue, which was diagnosed as infection of M. tuberculosis (Fuster et al., 2012).

4.4.3. Brain imaging

As reported by Silverman, there is increasing confidence in the use of PET/CT as a diagnostic tool for diagnosis of neurological conditions such as Alzheimer's disease (Silverman, 2004). Comparisons have been made of the relative ability of SPECT and PET to detect recurrent glioma (Which is a type of tumor that starts in

the brain or spine) after various clinical interventions. In a study comparing the effectiveness of ^{99}mTc- glucoheptonate (GH) SPECT/CT and^{18}F-FDOPA PET/CT for detection of recurrent glioma, it was identified that both provided equivalent diagnostic value though ^{99}mTc-GH SPECT/CT was more readily available and cheaper to use (Karunanithi et al., 2013).

Within the brain, there is an identified role for radionuclides that can be used to track concentration of glutamate receptors, which is the main excitatory neurotransmitter in the human brain. These receptors are potential targets in the treatment of many neurodegenerative and neuropsychiatric disorders (Majo et al., 2013). Therefore, this reflects the increasing trend to use PET/CT and SPECT /CT as areas where ^{99}mTc-GH SPECT/CT and ^{18}F-FDOPA PET/are readily available. With an ageing population, such diagnostic tools will play an increasing role in identification of various grades of dementia. In addition, such imaging technology has the ability to provide a valuable research tool to contribute in the development of new forms of medication where it was identified that the PET/CT and SPECT/CT images provide objective evidence of cognitive changes (Pupi et al., 2005).

While the main role of functional brain imaging is for the diagnosis of various presentations of dementia/Alzheimer's disease, there is also a requirement to diagnose Parkinson's disease, which is the second most frequently occurring cerebral degenerative disease, after Alzheimer disease. A study reported by Trott and Fakhri identifies the relative diagnostic performance of single isotope sequential SPECT (^{99}mTc), dual isotope simultaneous SPECT (^{99}-mTc/^{123}I) and PET (^{11}C-altropane) (Trott and El Fakhri, 2008). The highest diagnostic ranking was with PET, followed by simultaneous SPECT and then single isotope sequential SPECT. As a result, the use of PET and SPECT is being used as a diagnostic tool for identification and classification of neurological disorders. This reflects the increasing number of clinical specialties that are making use of PET/CT and SPECT/CT for both diagnosis of condition and disease management.

4.5. The limitations and capabilities of SPECT/CT and PET/CT

It is apparent that PET functionality is limited by short time scales of radionuclides such as ^{13}N and ^{15}O which essentially require on site cyclotron radionuclide production facilities. Therefore, developments in PET relating to these and similar radionuclides will be limited by funding resources. There is also a general appreciation have been described in Lewellen's review that developments in PET detector technology has the potential to further improve image quality and reduce image capture times. Such developments in detector technology are identified from areas of high-energy physics experiments (Lewellen, 2008).

The high number of scattered gamma ray photons associated with SPECT images, however, is identified as a factor limiting image quality. Specific techniques such as scatter correction techniques have been identified for minimising the effect of such scattering on image quality (Zaidi and Koral, 2004).

4.6. PET/MRI and SPECT/MRI: Challenges and difficulties

The integration of PET and SPECT with magnetic resonance imaging (MRI) provides both the opportunity and the challenge of integrating radioisotope imaging modalities with tissue-specific structural imaging technology. This flexibility within MRI is based on the ability to select scan parameters based on selected tissue characteristics, with the option of identifying of specific metabolic pathways. The characteristics of MRI technology, however, have major problems with high values of static magnetic fields (from MRI) and photomultiplier tubes, where the photomultiplier tubes must be kept far away from the magnet. One solution is to physically separate the MRI high magnetic field zone from the SPECT or PET zone and transport the patient using an extended rail between systems. Early developments in PET/SPECT/MRI systems used light guides or optical fibres to distance photomultiplier tubes from the MRI zone of high static magnetic field. More recently, however, hybrid PET/MRI systems have been developed that utilise avalanche photodiodes that are relatively immune to static magnetic field values. Moreover, the nature of the MRI technology, such as the superconducting magnetic field system and the radiofrequency amplifier systems, would significantly raise the cost of the hybrid PET/MRI system above that of the equivalent PET/CT facility, and therefore that might restrict the availability of such systems. In addition, the image acquisition time of MRI scans is significantly longer than that of CT scans and is likely to be the limiting factor determining scan time.

A recent experiment described an MRSPECT (SPECT/MRI) system where a cadmium-zinc-telluride (CZT) detector sub system was placed within an existing MRI scanner. It was identified that while satisfactory SPECT images could be obtained, the metallic components of the SPECT sub system introduced degradation in MRI image quality (Hamamura et al., 2010). However, a relevant review of the role of combined PET/MRI imaging for use in oncology, such as for tumour staging and lymph node assessment, has produced high-resolution images of whole body scan (Schmidt et al., 2007).

5. Conclusions and future developments

Nuclear medicine imaging technology can look back on an initial active phase with the invention of the anger camera technology and development of planar camera imaging, leading onto SPECT and eventually SPECT/CT. Nuclear medicine imaging is currently in a phase of rapid technological development where routine radioisotope scanning is now typically being undertaken using SPECT/CT technology and is becoming less of a specialist diagnostic facility. The basic technology of the planar gamma camera is still applicable to state of the art SPECT imaging technology currently available. The more recent rapid development phase of PET and PET/CT is still active and with improvements being identified in imaging quality as detection systems become faster. It is important, however, for physicists working with such technology in the clinical environment to appreciate the basics of operation of such systems. In the context of SPECT/CT and PET/CT technologies, however, a key difference between such imaging modes will be the nature of the uptake in the body of the carrier radioisotope pharmaceutical. Therefore, SPECT/CT technologies will maintain the advantage of imaging patients where uptake of radiopharmaceuticals takes place over several hours. Moreover, it is likely that there will be continuing developments of such technology to improve scan quality, reduce patient radiation dose from radionuclide (SPECT) and X-ray exposure from CT scanning and reduce scan time.

It was clear that there is a preference for systems, which provide PET/CT within a single scanning facility rather than separate PET and CT systems where images are fused from essentially different imaging systems. A key element of the software of such systems was the software function which fuses the two imaging data together. In addition, the further uptake of PET/CT is likely to be influenced by the availability of appropriate radiopharmaceuticals and where the development of mini cyclotrons as integral elements of PET/CT imaging system would significantly boost PET/CT imaging uptake. This is likely; however, to both increase capital and revenue requirements of such installations.

Nuclear medicine has established imaging technologies which provide key diagnostic information for patient management. It is

also identified that they provide a key research tool in the study of, for example, Alzheimer's disease and Parkinson's disease where the patient's status can be objectively related to potential drug treatments. Future developments in SPECT/CT and PET/CT imaging are also likely to be associated with detection system, the supplementary of radionuclides and new pharmaceutical preparations that target specific metabolic pathways.

Declaration of Competing Interest

The authors declare that they have no known competing financial interests or personal relationships that could have appeared to influence the work reported in this paper.

Acknowledgments

The author is thankful to the Deanship of Scientific Research at Najran University for funding this work under the National Research Priorities funding program (grant no NU/NRP/MRC/11/2).

References

Al Moudi, M., Sun, Z., Lenzo, N., 2011. Diagnostic value of SPECT, PET and PET/CT in the diagnosis of coronary artery disease: A systematic review. Biomed Imaging Interv. J. 7 (2), e9. Epub 2011 Apr 1.

Appelgren, L.K., 2020. Methods of recording tumor blood flow. In: Tumor Blood Circulation: Angiogenesis, Vascular Morphology and Blood Flow of Experimental and Human Tumors. CRC Press, pp. 87–101.

Avram, A.M., 2012. Radioiodine scintigraphy with SPECT/CT: an important diagnostic tool for thyroid cancer staging and risk stratification. J. Nucl. Med. 53 (5), 754–764.

Beekman, F., van der Have, F., 2007. The pinhole: gateway to ultra-high-resolution three-dimensional radionuclide imaging. Eur. J. Nucl. Med. Mol. Imaging 34 (2), 151–161.

Beller, G.A., Bergmann, S.R., 2004. Myocardial perfusion imaging agents: SPECT and PET. J. Nucl. Cardio l (11), 71–86.

Bhargava, P., He, G., Samarghandi, A., Delpassand, E.S., 2012. Pictorial review of SPECT/CT imaging applications in clinical nuclear medicine. Am. J. Nucl. Med. Mol. Imaging 2 (2), 221–231.

Blahd, W.H., 1996. Ben Cassen and the development of the rectilinear scanner. Semin. Nucl. Med. 26 (3), 165–170.

Cachovan, M., Vija, A.H., Hornegger, J., Kuwert, T., 2013. Quantification of 99mTc-DPD concentration in the lumbar spine with SPECT/CT. EJNMMI Res. 3 (1), 45. https://doi.org/10.1186/2191-219X-3-45.

Cherry, S., Sorenson, J., Phelps, M., 2012. Physics in Nuclear Medicine. Saunders, Philadelphia.

Chételat, G., Arbizu, J., Barthel, H., Garibotto, V., Law, I., Morbelli, S., Drzezga, A., 2020. Amyloid-PET and 18F-FDG-PET in the diagnostic investigation of Alzheimer's disease and other dementias. Lancet Neurol. 19 (11), 951–962.

Conti, M., 2011. Focus on time-of-flight PET: the benefits of improved time resolution. Eur. J. Nucl. Med. Mol. Imaging 38 (6), 1147–1157. https://doi.org/10.1007/s00259-010-1711-y. Epub 2011 Jan 13.

Cook, G.J.R., 2010. Miscellaneous indications in bone scintigraphy: metabolic bone diseases and malignant bone tumors. Semin. Nucl. Med. 40 (1), 52–61.

Crișan, G., Moldovean-Cioroianu, N.S., Timaru, D.G., Andrieș, G., Căinap, C., Chiș, V., 2022. Radiopharmaceuticals for PET and SPECT Imaging: A literature review over the last decade. Int. J. Mol. Sci. 23 (9), 5023.

de Leiris, N., Leenhardt, J., Boussat, B., Montemagno, C., Seiller, A., Phan Sy, O., Djaileb, L., 2020. Does whole-body bone SPECT/CT provide additional diagnostic information over [18F]-FCH PET/CT for the detection of bone metastases in the setting of prostate cancer biochemical recurrence? Cancer Imaging 20 (1), 1–11.

Di Carli, M.F., Dorbala, S., Meserve, J., El Fakhri, G., Sitek, A., Moore, S.C., 2007. Clinical myocardial perfusion PET/CT. J. Nucl. Med. 48 (5), 783–793.

Dilsizian, V., 2021. SPECT and PET myocardial perfusion imaging: Tracers and techniques. In: Atlas of Nuclear Cardiology. Springer, Cham, pp. 79–124.

Flotats, A., Knuuti, J., Gutberlet ,M., Marcassa, C., Bengel, F.M., Kaufmann, P.A., Rees, M.R. Hesse, B., 2011. Cardiovascular Committee of the EANM, the ESCR and the ECNC. Hybrid cardiac imaging: SPECT/CT and PET/CT. A joint position statement by the European Association of Nuclear Medicine (EANM), the European Society of Cardiac Radiology (ESCR) and the European Council of Nuclear Cardiology (ECNC). Eur. J. Nucl. Med. Mol. Imaging. 38(1):201–212.

Fuster, D., Solà, O., Soriano, A., Monegal, A., Setoain, X., Tomás, X., Garcia, S., Mensa, J., Rubello, D., Pons, F., 2012. A prospective study comparing whole-body FDG PET/CT to combined planar bone scan with 67Ga SPECT/CT in the Diagnosis of Spondylodiskitis. Clin. Nucl. Med. 37 (9), 827–832.

Gaemperli, O., Bengel, F.M., Kaufmann, P.A., 2011. Cardiac hybrid imaging. Eur. Heart J. 32 (17), 2100–2108.

Go, R.T., Marwick, T.H., MacIntyre, W.J., et al., 1990. A prospective comparison of rubidium-82 PET and thallium-201 SPECT myocardial perfusion imaging utilizing a single dipyridamole stress in the diagnosis of coronary artery disease. J. Nucl. Med. 31, 1899–1905.

Gramuglia, F., Frasca, S., Ripiccini, E., Venialgo, E., Gâté, V., Kadiri, H., Descharmes, N., Turover, D., Charbon, E., Bruschini, C., 2021. Light Extraction Enhancement Techniques for Inorganic Scintillators. Crystals 11 (4), 362. https://doi.org/10.3390/cryst11040362.

Hachamovitch, R., Johnson, J.R., Hlatky, M.A., Cantagallo, L., Johnson, B.H., Coughlan, M., et al., 2009. The study of myocardial perfusion and coronary anatomy imaging roles in CAD (SPARC): design, rationale, and baseline patient characteristics of a prospective, multicenter observational registry comparing PET, SPECT, and CTA for resource utilization and clinical outcomes. J. Nucl. Cardiol. 16, 935–948.

Hamamura, M.J., Ha, S., Roeck, W.W., Muftuler, L.T., Wagenaar, D.J., Meier, D., Patt, B. E., Nalcioglu, O., 2010. Development of an MR-compatible SPECT system (MRSPECT) for simultaneous data acquisition. Phys. Med. Biol. 55 (6), 1563–1575.

Ho, C.L., Chen, S., Ho, K.M., Chan, W.K., Leung, Y.L., Cheng, K.C., Wong, K.N., Cheung, M.K., Wong, K.K., 2012. Dual-tracer PET/CT in renal angiomyolipoma and subtypes of renal cell carcinoma. Clin. Nucl. Med. 37 (11), 1075–1082.

Jinzaki, M., Tanami, Y., Yamada, M., Kuribayashi, S., 2011. Progress and Current State of Coronary CT. Ann. Vasc. Dis. 4 (1), 7–18.

Johnson, K.A., Nick, C., Fox, N.C., Sperling, R.A., Klunk, W.E., 2012. Brain Imaging in Alzheimer Disease. Cold Spring Harb. Perspect. Med. 2, (4). https://doi.org/10.1101/cshperspect.a006213 PMCID: PMC3312396 a006213.

Jora, C., Mattakarottu, J.J., Aniruddha, P.G., Mudalsha, R., Singh, D.K., Pathak, H.C., Sharma, N., Sarin, A., Prince, A., Singh, G., 2011. Comparative evaluation of 18F-FDOPA, 13N-AMMONIA, 18F-FDG PET/CT and MRI in primary brain tumors - A pilot study. Indian. J. Nucl. Med. 26 (2), 78–81. https://doi.org/10.4103/0972-3919.90256.

Juarez-Orozco, L.E., Cruz-Mendoza, J.R., Guinto-Nishimura, G.Y., Walls-Laguarda, L., Casares-Echeverría, L.J., Meave-Gonzalez, A., Alexanderson, E., 2018. PET myocardial perfusion quantification: Anatomy of a spreading functional technique. Clin. Transl. Imag. 6 (1), 47–60.

Karunanithi, S., Bandopadhyaya, G.P., Sharma, P., Kuma, A., Singla, S., Malhotra, A., Gupta, D.K., Bal, C., 2013. Prospective Comparison of 99mTc-GH SPECT/CT and 18F-FDOPA PET/CT for Detection of Recurrent Glioma: A Pilot Study. Clin. Nucl. Med. [Epub ahead of print].

Kharfi, F., 2013. Principles and Applications of Nuclear Medical Imaging: A Survey on Recent Developments. Imaging and Radioanalytical Techniques in Interdisciplinary Research - Fundamentals and Cutting Edge Applications, INTECH.

Kobylecka, M., Mączewska, J., Fronczewska-Wieniawska, K., Mazurek, T., Płazińska, M.T., Królicki, L., 2012. Myocardial viability assessment in 18FDG PET/CT study (18FDG PET myocardial viability assessment). Nucl. Med. Rev. Cent. East. Eur. 15 (1), 52–60. https://doi.org/10.5603/nmr-18731.

Lewellen, T.K., 2008. Recent developments in PET detector technology. Phys Med Biol. 53 (17), R287–R317.

Lodge, M.A., Braess, H., Mahmoud, F., Jongdae Suh, J., Nancy Englar, N., Geyser-Stoops, S., Jason Jenkins, J., Bacharach, S.L., Dilsizian, V., 2005. Developments in Nuclear Cardiology: Transition from Single Photon Emission Computed Tomography to Positron Emission Tomography/Computed Tomography. J. Invasive Cardiol. 17 (9), 491–496.

Machac, J., 2007. Radiopharmaceuticals for Clinical Cardiac PET Imaging in Cardiac PET and PET/CT Imaging. Springer, Berlin.

Madsen, M.T., 2007. Recent advances in SPECT imaging. J. Nucl. 48, 661–673.

Majo, V.J., Prabhakaran, J., Mann, J.J., Kumar, J.S., 2013. PET and SPECT tracers for. Drug Discov. Today 18 (3–4), 173–184.

McKillop, J.H., 1980. Thallium 201 scintigraphy. West. J. Med. 133 (1), 26–43.

Mosci, C., Pericole, F.V., Oliveira, G.B., Delamain, M.T., Takahashi, M.E., Carvalheira, J. B.C., Ramos, C.D., 2020. 99mTc-sestamibi SPECT/CT and 18F-FDG-PET/CT have similar performance but different imaging patterns in newly diagnosed multiple myeloma. Nucl. Med. Commun. 41 (10), 1081.

Moses, W.W., 2007. Recent Advances and Future Advances in Time-of-Flight PET. Nucl. Instrum. Methods Phys. Res. A. 580 (2), 919–924.

Nair, V.S., Keu, K.V., Luttgen, M.S., Kolatkar, A., Vasanawala, M., Kuschner, W., Bethel, K., Lagaru, A.H., Hoh, C., Shrager, J.B., Loo Jr, B.W., Bazhenova, L., Nieva, J., Gambhir, S.S., Kuhn, P., 2013. An Observational Study of Circulating Tumor Cells and (18)F-FDG PET Uptake in Patients with Treatment-Naive Non-Small Cell Lung Cancer. PLoS One 8 (7), e67733.

Naya, M., Di Carli, M.F., 2010. Myocardial perfusion PET/CT to evaluate known and suspected coronary artery disease. Q. J. Nucl. Med. Mol. Imaging 54 (2), 145–156.

Oh, J.R., Byun, B.H., Hong, S.P., Chong, A., Kim, J., Yoo, S.W., Kang, S.R., Kim, D.Y., Song, H.C., Bom, H.S., Min, J.J., 2011. Comparison of ^{131}I whole-body imaging, ^{131}I SPECT/CT, and ^{18}F-FDG PET/CT in the detection of metastatic thyroid cancer. Eur. J. Nucl. Med. Mol. Imaging 38 (8), 1459–1468.

Philips, 2010, Clinical case study collection Philips. BrightView XCT nuclear medicine system. Available at: http://www.citiscan.com.au/sites/all/themes / scr/pdf/INFO-GUIDE-Philips-BrightView-XCT-Nuclear-Medicine-Case-Studies. pdf. [Accessed at 15 Nov 2022].

Piccard, D, 2005, *Notes* in modern physics and ionizing radiation. Available at: http://www.ohio.edu/people/piccard/radnotes/detectors.html. [Accessed in 11 Nov 2022].

Pupi, A., Mosconi, L., Nobili, F.M., Sorbi, S., 2005. Toward the validation of functional neuroimaging as a potential biomarker for Alzheimer's disease: implications for drug development. Mol. Imag. Biol. 7 (1), 59–68.

Rager, O., Lee-Felker, S.A., Tabouret-Viaud, C., Felker, E.R., Poncet, A., Amzalag, G., Walter, M.A., 2018. Accuracy of whole-body HDP SPECT/CT, FDG PET/CT, and their combination for detecting bone metastases in breast cancer: an intra-personal comparison. Am. J. Nucl. Med. Mol. Imaging 8 (3), 159.

Rahmim, A., Zaidi, H., 2008. PET versus SPECT: strengths, limitations and challenges. Nucl. Med. Commun. 29 (3), 193–207.

Rischpler, C., Higuchi, T., Fukushima, K., Javadi, M.S., Merrill, J., Nekolla, S.G., Bravo, P.E., Bengel, F.M., 2012. Transient ischemic dilation ratio in 82Rb PET myocardial perfusion imaging: normal values and significance as a diagnostic and prognostic marker. J. Nucl. Med. 53 (5), 723–730. https://doi.org/10.2967/jnumed.111.097600. Epub 2012 Apr 9.

Santos, B.S., Ferreira, M.J., 2019. Positron emission tomography in ischemic heart disease. Rev. Port. Cardiol. 38 (8), 599–608.

Schelbert, H.R., Wisenberg, G., Phelps, M.E., et al., 1982. Noninvasive assessment of coronary stenoses by myocardial imaging during pharmacologic coronary vasodilation. VI. Detection of coronary artery disease in human beings with intravenous N-13 ammonia and positron computed tomography. Am. J. Cardiol. 49 (5), 1197–1207.

Schirrmeister, H., Glatting, G., Hetzel, J., Nussle, K., Arslandemir, C., Buck, A., Dziuk, K., Gabelmann, A., Reske, S.N., Hetzel, M., 2001. Prospective Evaluation of the Clinical Value of Planar Bone Scans, SPECT, and 18F-Labeled NaF PET in Newly Diagnosed Lung Cancer. J. Nucl. Med. 42 (12), 100–104.

Schmidt, G.P., Kramer, H., Reiser, M.F., Glaser, C., 2007. Whole-body magnetic resonance imaging and positron emission tomography-computed tomography in oncology. Top. Magn. Reson. Imaging 18 (3), 193–202.

Shukla, A.K., Kumar, U., 2006. Positron emission tomography: An overview. J. Med. Phys. 31 (1), 13–21. https://doi.org/10.4103/0971-6203.25665.

Silverman, D., 2004. Brain FDG-PET in the Diagnosis of Neurodegenerative Dementias: Comparison with Perfusion SPECT and with Clinical Evaluations lacking Nuclear Imaging. J. Nucl. Med. 45 (4), 594–607.

Stewart, R.E., Schwaiger, M., Molina, E., et al., 1991. Comparison of rubidium-82 positron emission tomography and thallium-201 SPECT imaging for detection of coronary artery disease. Am. J. Cardiol. 67, 1303–1310.

Trott, C.M., El Fakhri, G., 2008. Sequential and simultaneous dual-isotope brain SPECT: comparison with PET for estimation and discrimination tasks in early Parkinson disease. Med. Phys. 35 (7), 3343–3353.

University of Virginia, 2012, PET/CT Basic [online] Available at http://www.med-ed.virginia.edu/courses/rad/PETCT/attenuation.html# [Accessed 15 Nov 2022].

Varoquaux, A., Rager, O., Lovblad, K.O., Masterson, K., Dulguerov, P., Ratib, O., Becker, C.D., Becker, M., 2013. Functional imaging of head and neck squamous cell carcinoma with diffusion-weighted MRI and FDG PET/CT: quantitative analysis of ADC and SUV. Eur. J. Nucl. Med. Mol. Imaging 40 (6), 842–852.

Veit-Haibach, P., Kuhn, F.P., Wiesinger, F., Delso, G., von Schulthess, G., 2013. PET-MR imaging using a tri-modality PET/CT-MR system with a dedicated shuttle in clinical routine. MAGMA 26 (1), 25–35. https://doi.org/10.1007/s10334-012-0344-5. Epub 2012 Oct 9 PMID: 23053712.

Wang, J., Jin, C., Zhou, J., Zhou, R., Tian, M., Lee, H.J., Zhang, H., 2022. PET molecular imaging for pathophysiological visualization in Alzheimer's disease. Eur. J. Nucl. Med. Mol. Imaging, 1–19.

Zaidi, H., Koral, K.F., 2004. Scatter modelling and compensation in emission tomography. Eur. J. Nucl. Med. Mol. Imaging 31, 761–782.